SIMPLIFIED DESIGN METHOD FOR A SYMMETRICAL WING-BODY FAIRING

C.B. Steenaert, B.W. van Oudheusden, L.M.M. Boermans
Faculty of Aerospace Engineering, Delft University of Technology
Email: B.W.vanOudheusden@lr.tudelft.nl

Keywords: *wing-body juncture, fairing design*

Abstract

A simplified procedure is presented for the design of a symmetrical wing-body fairing. The design aims at optimizing the design of the fairing, which is to serve the twofold purpose of eliminating the separation near the wing body junction, as well as minimizing leading edge contamination of the laminar wing. The design optimization procedure is based on the analysis of the viscous-flow performance of a fairing of prescribed geometry. First, a panel method is used to determine the inviscid flow around the fairing. This is then followed by an integral-method calculation of the boundary layer development on the attachment line along the body and the fairing, so only in the symmetry plane of the flow. As an application a fairing was designed for a straight NACA0015-wing mounted on a flat plate. Tests in the wind tunnel confirmed the effectiveness of the fairing.

1 General Introduction

1.1 Background

Modern high-performance sailplanes are designed to operate at the top of aerodynamic efficiency, with extensive-laminar-flow wings and optimized fuselage design. In this context the wing-body junction remains a point of significant concern. Simply attaching the (straight) wing to the fuselage will cause a large separation region near the junction, where the fuselage boundary layer encounters the strong pressure rise of the wing stagnation region. The common measure to eliminate this separation is by applying a fairing of suitable shape at the junction. In the present context there is a second consideration in the design of the fairing, namely that of the contamination of the laminar wing by the turbulent boundary layer on the fuselage.

Because of the complex flow structure that occurs near a wing-body junction, the determination of the fairing shape has traditionally been a design art relying heavily on experience, and (experimental) trial and error, see e.g. [1-4]. Some recent CFD studies have handled fairing design on the basis of Navier-Stokes computations [5]. Evidently, the amount of computing effort required for such an approach is very large, which makes it too demanding for routine design applications. Also, flow relaminarization is not yet within the capabilities of standard CFD.

1.2 Preliminary design considerations

In this study a simplified design procedure is proposed, which in its present form can be applied to symmetrical flow situations. It is based on a classical boundary layer approach.

First, the inviscid flow is determined for a proposed fairing geometry with a panel method. The relevant properties of the inviscid pressure distribution are then supplied to a boundary layer computation, to assess the viscous-flow performance of the fairing. Although this approach would evidently be incorrect for flows with large separation, as in the case of the junction without fairing, the design aim is a fairing without separation, for which there is a reasonable justification of this approach.

A second important simplifying aspect of the procedure is that the boundary layer development is computed only on the dividing

streamline along the plate and the fairing leading edge. It is assumed that this is sufficiently representative of the performance of the fairing as a whole. In the case of a symmetrical flow geometry, the flow in the plane of symmetry can indeed be determined without the need of considering the spanwise dimension [6]. A quasi-2D boundary layer computation along the central streamline then suffices, for which standard 2D-methods need to be extended to take the lateral flow relieving effect into account [7]. In the present study Head's turbulent entrainment method was used [8]. The computation yields the development of the boundary layer shape factor and momentum thickness, which are used to assess separation and relaminarization by semi-empirical criteria.

These computational tools can then be applied to study the effect of altering the shape and dimensions of the fairing and, thus, to optimize it in terms of the design requirements.

2 Flow Analysis

The design procedure that is developed in the present study is based on a classical boundary layer approach, and exploits the simplifications that apply in a symmetrical flow situation. A symmetrical wing is considered under zero angle of attack, while the fuselage is modeled as a flat plate. Incompressible flow is assumed and the incoming boundary layer on the plate is taken to be turbulent as in real applications.

As shown elsewhere in more detail [6, 7, 9], it is possible to determine the boundary layer development in the symmetry plane alone, such that only the flow along the attachment line has to be analyzed. The attachment line is the streamline that will either end in the stagnation point in case of a wing without sweep or the streamline that follows the leading edge of the wing towards the tip. In case of the simplified configuration presented above the attachment line is the intersection line between the plane of symmetry and the flat plate, the fairing and the wing leading-edge surface. It is expected that the steepest adverse pressure gradient will occur along the attachment line and that as a result the most upstream separation location is on this line. To prevent separation in front of the wing, it can be concluded that it is necessary that no separation takes place on the attachment line.

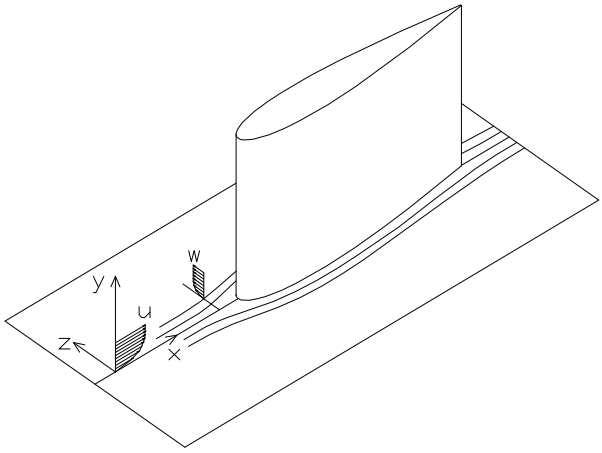

Figure 1: Basic geometry of a wing-body junction and coordinate system

The coordinate system is taken as shown in Fig. 1, where initially on the plate the *x*-axis is in the direction of the free-stream, the *y*-axis is normal to the plate and *z*-axis is in the lateral direction along the plate, and normal to the symmetry plane of the configuration.

The viscous flow equations governing the boundary layer development are used in a body-fitted coordinate frame: *x* follows the flow along the surface in the symmetry plane, *y* is normal to the local surface and *z* is in the lateral direction, normal to both *x* and *y*. The corresponding velocity components are *u*, *v* and *w*. Extension of this coordinate system onto the wing means that *x* follows the wing leading edge in spanwise direction.

2.1 Boundary layer in the symmetry plane

For reasons of symmetry, the lateral velocity component *w* is zero at the symmetry plane, and must be replaced by its lateral gradient, $\tilde{w} = \partial w / \partial z$ as primary variable. The equations governing the boundary layer flow in the symmetry plane ($z = 0$), are then given by the continuity equation, the *x*-momentum equation and the *z*-derivative of the *z*-momentum equation, cf. [6, 11]. These equations allow the calculation of the boundary layer development in the symmetry plane alone, as the lateral spatial dimension is absent in them. As matching conditions with the inviscid free-

stream, only the values of U_e and $\tilde{W}_e$ at the edge of the boundary layer are required as function of x. These are to follow from an inviscid flow calculation for the complete plate-fairing-wing combination.

2.2 Effect of the fairing on the junction flow

Some typical aspects of the junction flow are highlighted here, to illustrate how the fairing functions in eliminating the flow separation at the wing-body junction, and how the inviscid flow conditions are involved in this process.

In the absence of a fairing (as in Fig. 1) the geometrical discontinuity at the leading edge of the junction creates a stagnation point in the inviscid flow. As a result of this pressure rise, the viscous flow will separate. Approaching the stagnation point of the 3-D configuration, lateral outflow out of the symmetry plane will occur, i.e. $\tilde{W}_e > 0$. This is an illustration of the well-known 3-D 'flow-relieving' effect. Although this effect will reduce the boundary layer growth and delay separation in comparison to a 2-D flow subjected to the same streamwise pressure gradient, this effect is clearly insufficient to prevent separation. Massive separation occurs, giving rise to a complex separated flow field [10].

The function of the fairing can now be seen in the above perspective, in that it makes the pressure rise less severe and that the lateral outflow will start earlier, further upstream. The objective (in case of a non swept wing) is to empty the boundary layer on the attachment line that much, that the boundary layer will be totally empty at the point where the flow stagnates. It may be obvious that increasing the size of the fairing will progressively enhance this process. When considering the viscous flow, i.e. the fuselage boundary layer, it is evident that any flow turbulence on the plate will be transported onto the fairing as well. However, the local Reynolds number of the viscous flow will decline rapidly as both the outer velocity and the boundary layer thickness decrease. It will ultimately become so low that the turbulence decays completely and laminarization of the flow occurs [11, 12]. It can be understood that the second design requirement, which is minimum contamination of the (laminar) wing, requires a rapid laminarization. This is served by reducing the size of the fairing. In case of a big fairing, the turbulent flow can continue up to a higher point above the flat plate on the fairing. A small steep fairing will have an almost stagnated flow in front of it whereby the lateral outflow is very severe. As a result, the local Reynolds number will decrease very rapidly.

A second reason to make the fairing as small as possible is to reduce the wetted area of the fairing. Hereby, the drag decreases occurring from skin friction. The fairing however has to be large enough to prevent separation of the flow by relaxing the pressure rise and promoting the lateral flow.

2.3 Integral boundary layer calculation

For the boundary layer calculation an integral method is used, for which Head's entrainment method [8] was adapted to take the extra flow relieving effect into account. This leads to the following basic relations [9], which are the integral streamwise momentum equation and the entrainment equation:

$$\frac{dq}{dx} = \frac{C_f}{2} - (2+H)\frac{q}{U_e}\frac{dU_e}{dx} - \frac{\tilde{W}_e}{U_e}\int_0^d \frac{\tilde{w}}{\tilde{W}_e}\left(1-\frac{u}{U_e}\right)dy \quad (1)$$

$$\frac{1}{U_e}\frac{d}{dx}(U_e q H_1) = C_E - \frac{\tilde{W}_e}{U_e}\int_0^d \frac{\tilde{w}}{\tilde{W}_e}dy \quad (2)$$

In these equations all boundary layer parameters have their usual meaning and are related to the streamwise velocity profile. As the flow in the symmetry plane is planar, the assumption is made that the closing relations for 2-D flow can be applied [13]. In particular, Head's correlations are used for the shape factor $H_1 = (d\text{-}d^*)/q$ and the entrainment rate;

$$C_E = F(H_1) = 0.0306(H_1-3)^{-0.653}$$
$$H_1 = 1.535(H-0.7)^{-2.715} + 3.3 \quad (3)$$

and White's skin-friction law [13]:

$$C_f \approx \frac{0.3e^{-1.33H}}{(\log_{10}\mathrm{Re}_q)^{1.74+0.31H}} \quad (4)$$

2.4 Modeling of the cross-flow terms

Next, also the cross-flow terms need to be modeled. These express the integrated lateral flow-relieving effect, in terms of a lateral transport of momentum-deficit in Eq. (1) and of mass in the boundary layer in Eq. (2). Both terms are seen to reduce the boundary layer growth when $\tilde{w} > 0$, as expected. One option to model these terms would be to determine the cross-flow with an additional equation, typically the integral form of the lateral momentum equation. Indeed such an approach is common to many 3-D integral methods and was also applied by Cumpsty and Head [7].

In the present analysis, an even simpler approach is proposed to the cross-flow term, relying on the typical flow configurations that occur in the present application. The streamwise velocity profile will decelerate due to an adverse pressure gradient, whereas the lateral direction of the flow is accelerated from the symmetry plane outwards. Therefore, it can be assumed that the *w*-profile is fuller than the *u*-profile, so:

$$\frac{u}{U_e} \le \frac{\tilde{w}}{\tilde{W}_e} \le 1 \qquad (5a)$$

This may be generalized by proposing:

$$\frac{\tilde{w}}{\tilde{W}_e} = r + (1-r)\frac{u}{U_e}, \quad 0 \le r \le 1 \qquad (5b)$$

Now the two limiting assumptions can be considered:

Assumption 1: $\frac{\tilde{w}}{\tilde{W}_e} \approx \frac{u}{U_e} \quad (r = 0)$ (6a)

Assumption 2: $\frac{\tilde{w}}{\tilde{W}_e} \approx 1 \quad (r = 1)$ (6b)

It is clear that assumption 1 will be a conservative estimate, which underrates the lateral flow relieving, while on the other hand assumption 2 may be too optimistic, in that it overestimates this effect. If both assumptions are considered separately, the outcome is expected to give the typical range for the boundary layer properties, like the shape factor and the momentum loss thickness, and the correct solution is expected to be somewhere in between. Once the cross-flow effect becomes important, which is when approaching the fairing, the adverse pressure gradient will have become appreciable as well. Under this condition, where the velocity of the flow rapidly decreases, the second equality is probably a better approximation than the first.

The adoption of either assumption allows the integrals in Eqs. (1) and (2) to be expressed in terms of the streamwise velocity profile:

$$\frac{dq}{dx} = \frac{C_f}{2} - (2+H)\frac{q}{U_e}\frac{dU_e}{dx} - \frac{\tilde{W}_e}{U_e}(rH + 1 - r)q \qquad (7)$$

$$\frac{1}{U_e}\frac{d}{dx}(U_e\, q\, H_1) = F(H_1) - \frac{\tilde{W}_e}{U_e}(rH + H_1)q \qquad (8)$$

2.5 Relaminarization Criterion

As discussed, the turbulent fuselage boundary layer extends onto the fairing and will ultimately relaminarize. One of the purposes of the fairing design is to establish laminar flow on the wing as close as possible to the wing-root.

Important evidence to quantify this relaminarization can be obtained from the behavior of the boundary layer on a swept-wing. The stability of the boundary layer at the wing attachment line is directly of relevance to the phenomenon of leading edge contamination. This effect was first discovered in the 1950's when attempts to realize natural laminar flow on swept wings were found to be hindered by turbulence traveling along the leading edge. Pioneering work in this field was performed by Pfenninger [11, 16], Gaster [14] and Poll [15], amongst others. Leading edge contamination causes the wing to become fully turbulent before the condition of linear instability of the laminar flow is reached. This premature transition is triggered by large initial disturbances, in particular the turbulence in the fuselage boundary layer at the wing root, which propagates and contaminates the attachment line boundary layer in spanwise direction.

One of the first to report and investigate this phenomenon was Pfenninger [21], who observed when testing the 30° swept X-21 wing that the flow on the inner part of the wing was turbulent over the full chord, but full chord laminar over the outer part of the wing. When

investigating the effect of disturbances at the attachment line in more detail, a marked influence of the value of $Re_{q,al}$, the momentum Reynolds number at the attachment line, was found. When $Re_{q,al}$ was smaller than 90 only a chordwise turbulent wedge developed downstream of an attachment line roughness (Fig. 2).

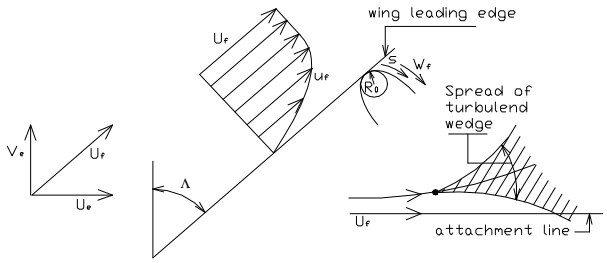

Figure 2: Leading edge contamination

Between 90 and 105, the spread became larger and turbulent bursts developed on the wing leading edge. Above the value of 105, the attachment line became fully turbulent.

A turbulent attachment line flow will act at every position along the leading edge as a source of turbulence, comparable to a local roughness element, which makes the flow turbulent over the full chord. As found by Pfenninger the turbulence can only propagate in spanwise direction when Re_q is larger than about 100. When this value falls below the critical threshold of around 100, contamination of the leading edge is ended. Similar values for this phenomenon were reported from experiments by Gaster [15], Poll [16], Cumpsty and Head [9] and from the DNS simulations by Spalart [17].

The situation on the fairing is similar to that on the swept-wing, and it is therefore assumed that the critical value of Re_q = 100 can be used as an indication of the location of relaminarization on the fairing. The exact value of this threshold may not be very critical, as Re_q decreases precipitously on the fairing as can be seen later in paragraph 3.3. Also, the method is primarily used to compare the performance of different fairing shapes.

3 Fairing Design

The fairing design method was applied to a (symmetrical) test configuration of a straight wing with a NACA 0015 section mounted on a flat plate. The design conditions were taken to resemble a sailplane configuration under normal flight conditions. The wing chord was chosen as 0.75 *m* and starting conditions for the boundary layer were prescribed at the position 0.5 *m* upstream of the (original) wing leading edge.

3.1 Definition of the fairing geometry

The fairing is formed by stretching the segment of the wing airfoil in front of the point of maximum thickness (at 30% chord), see Fig. 3.

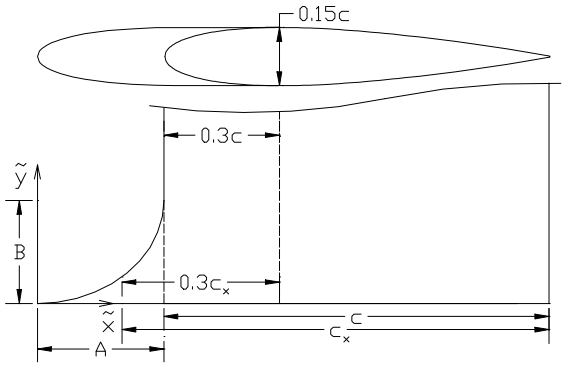

Figure 3: Fairing geometry

As the thickness distribution of the NACA 4-digit airfoil series is described analytically [18], this stretching can be carried out easily and accurately. The fairing shape is now defined by prescribing the leading edge curve in the symmetry plane. In the present investigation this was taken as an ellipse which is tangent to both the plate and the wing leading edge, with length *A* and height *B*. Now the fairing shape is completely determined by prescribing values for *A* and *B*.

3.2 Inviscid flow calculation

The inviscid flow around the wing-plate junction with fairing was determined by means of the panel program KK-AERO [19]. For the computations the plate needed to be modeled as a thin flat fuselage, which extends four chord lengths upstream of the wing and three chord lengths downstream of it, and with a width of four chord lengths. The height (semi-span) of the wing was eight chord lengths. The relevant data that are required for the boundary layer

calculations are the streamwise velocity U_e and the lateral velocity gradient $\tilde{W}_e$, at the surface in the plane of symmetry (the attachment line).

3.3 Boundary layer calculation

The starting conditions for the boundary layer computations were chosen such as to simulate the boundary layer development over the sailplane fuselage upstream. An initial value for the shape factor was chosen as H = 1.4 (a typical value for flat plate flow). To obtain a realistic value for the initial momentum thickness, the upstream length was modeled as a 2 *m* long flat plate with transition at 1.5 *m*. In case of the assumed fuselage, 1.5 *m* is the location of the widest cross section, see Fig. 4.

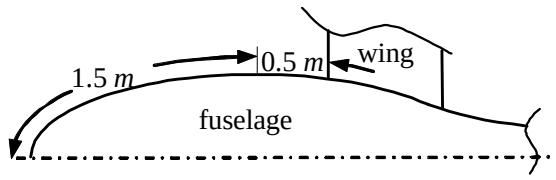

Figure 4: Sailplane fuselage-wing assumptions

Standard relations for the flat-plate boundary layer [13], yield a starting value of q = 0.695 *mm* at U_∞ = 20 *m/s*, and q = 0.439 mm at U_∞ = 50 *m/s*. Corresponding values of Re_q are 950 and 1500, respectively. The calculation is stopped when either separation is reached (H = 3), or when Re_q has dropped below the laminarization threshold (Re_q = 100).

3.4 Fairing optimization

The performance of the fairing can now be analyzed in relation to the values of A and B. As mentioned, the two basic requirements the fairing has to fulfill are that no separation takes place and that the boundary layer has to become laminar as close as possible to the wing-root. For a particular fairing the inviscid flow was determined with the panel method. Then boundary layer calculations were performed, comparing the two different assumptions for the cross-flow effect, for two typical values of the free-stream velocity (20 and 50 *m/s*).

The closeness of the viscous flow to separation is assessed on the basis of the value of the shape factor H. When using the conservative estimate of the cross-flow effect, Eq. (6a), separation was considered to be prevented if H did not exceed 3. For the other assumption, which overestimates the cross flow effect, some safety margin was incorporated in the design, in requiring that H was not to exceed a value of 2.25 on the fairing. Relaminarization was assumed to occur when Re_q falls below 100.

The optimum fairing size was determined by a selective exploration of the (A, B)-space. Varying the length A of the fairing shows that a minimum length is required to prevent separation and that the longer the fairing the lower the maximum value of H. For a given length, there is a (shallow) optimum for the height B in terms of preventing separation, as interpreted from the lowest value of maximum H. In the same way, the laminarization height was found to increase with both A and B.

Based on above considerations two optimal fairing shapes were selected. With the conservative approach a fairing was designed with A = 0.21c and B = 0.175c, while with the optimistic approach a smaller fairing was obtained with A = 0.14c and B = 0.20c, hence, one third shorter, but slightly higher.

Results of the boundary calculations for the smaller fairing are shown in Fig. 5. Here, x_f is the distance along the surface, with x_f = 0 indicating the beginning of the fairing. The top diagrams show the prescribed outer flow conditions, and the other three some typical boundary layer parameters. The skin friction coefficient $C_f = (t_x)_{wall} / \frac{1}{2} r U_\infty^2$ given here, is defined with the constant upstream velocity U_∞, rather than the local edge velocity U_e, in order to represent the absolute value of the skin friction. As shown by the calculations, initially the shape factor increases and the skin friction decreases, but on the fairing this development is reversed. Clearly it can be seen that with the conservative cross-flow assumption (6a), H becomes larger than 3, and the flow separates. With the optimistic cross-flow assumption (6b) the flow remains attached, whilst an increase of the flow speed is seen to reduce the risk of separation, but it delays the laminarization.

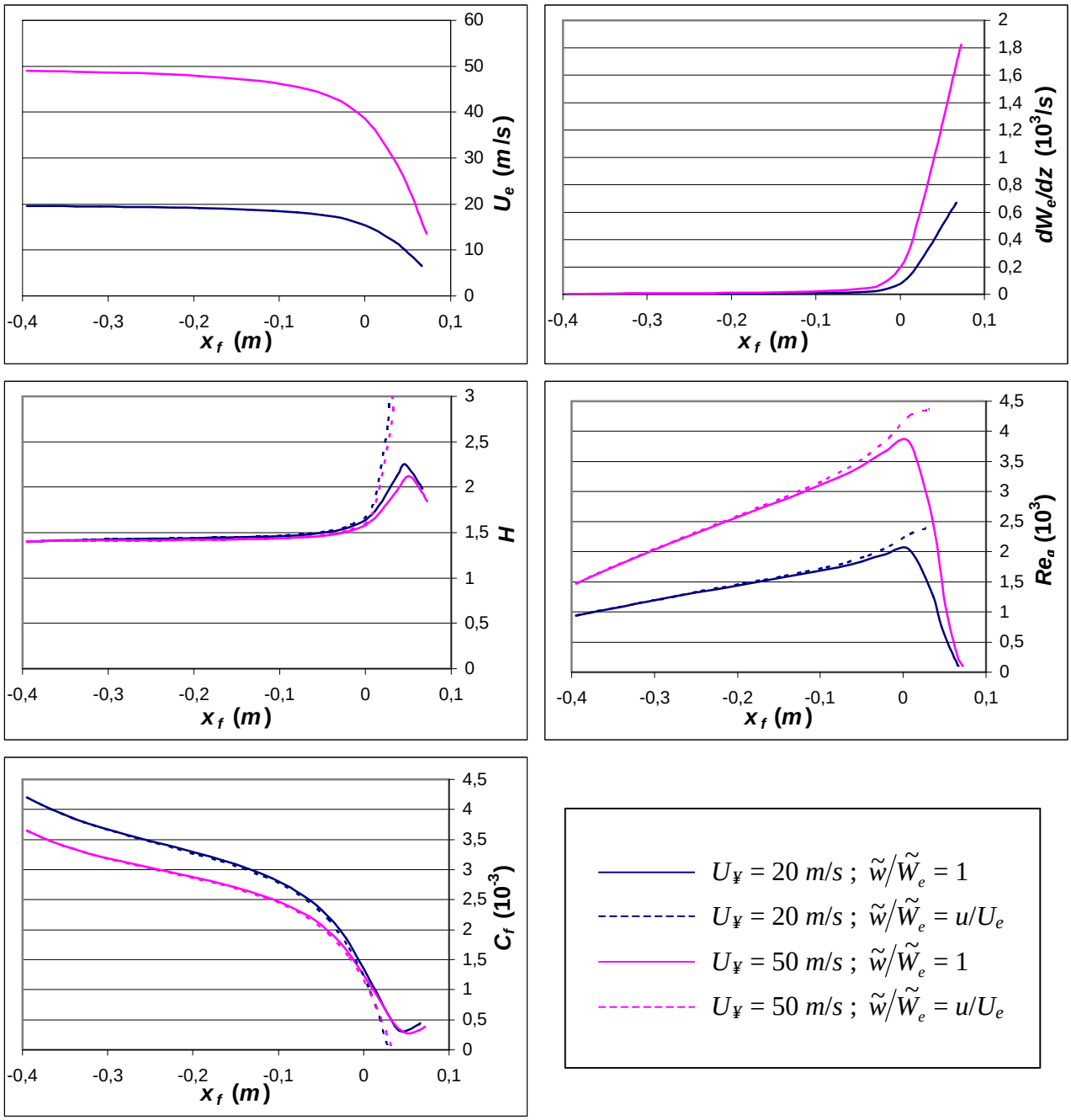

Figure 5: Computed boundary development for the small fairing (A = 0.14c, B = 0. 20c), with the effect of free-stream velocity and cross-flow modelling

3.5 Testing the fairing in the wind tunnel

The two fairing designs were tested in the test section (1.80 *m* x 1.25 *m*) of the Subsonic Low Turbulence Tunnel of the Delft University of Technology (Fig. 6).

A flat plate was installed which spans the width of the test section. A flap at the trailing edge was used to establish a zero pressure gradient on the flat plate, in the absence of the wing, which was verified by means of pressure taps in the plate.

The wing was mounted on the plate and fitted with a spanwise zigzag tape at the position of its maximum thickness, in order to trip the boundary layer there, and prevent separation of

the laminar boundary layer. The reason for this was that the primary concern of the present investigation is the flow at the front of the wing in order to evaluate the effectiveness of the fairing. Flow separation further downstream may disturb a proper assessment of this aspect of the flow, and should be eliminated in a realistic design by a suitable shape of the actual wing cross-section.

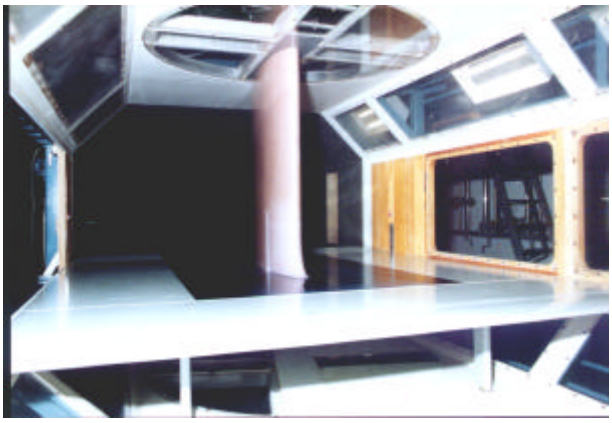

Figure 6: Plate-wing model in the wind tunnel

The starting conditions 0.5 *m* in front of the wing leading edge were adjusted to have the same momentum loss thickness as used in the calculations. This was done by applying zigzag tape onto the flat plat, such that the correct starting conditions were realized. This was verified by measuring the boundary layer profile with a small total pressure tube.

First the straight wing without any fairing was tested. Surface streamlines were visualized by applying a pigmented oil mixture on the wing and the flat plate. Tests at a free-stream speed of 20 *m/s* display the usual picture (see Fig. 7, left), with the plate boundary layer separating in front of the wing. The S-shaped streamlines reveal that a vortex is formed which wraps itself around the wing-root.

Next, both fairings were tested, the large fairing first. Some care was needed in visualizing the surface streamlines on the fairing, as the oil disappeared very rapidly around the wing root. Looking only at the end result of the oil pattern, this empty region may have been mistaken for a separation region. However, when the oil was applied near the wing root while the tunnel was running, streamlines could indeed be seen, moving the oil downstream in a few seconds. The cause of this was the increase in wall friction on the fairing as the boundary layer thickness decreases rapidly and the boundary layer becomes laminar on the fairing. This was also shown by the results of the boundary layer calculations (Fig. 5). As shown in Fig. 7 in the right picture (which displays the small fairing), streamlines can be observed all over the surface, indicating that the flow remains attached. This was verified by moving a small wool tuft just above the surface of the wing and the flat plate.

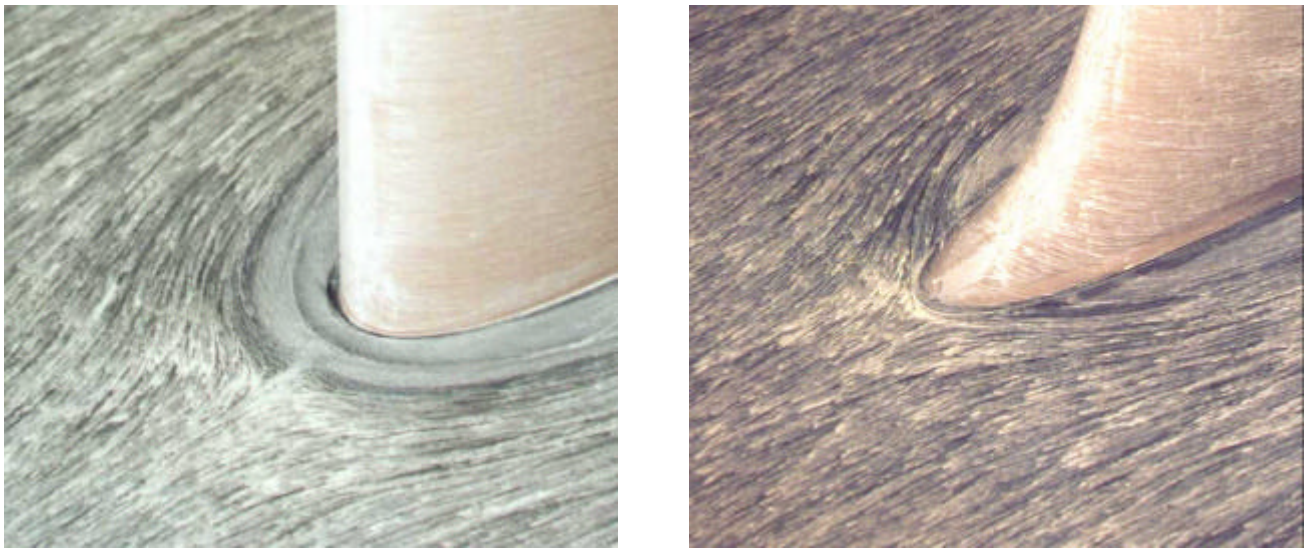

Figure 7: Effect of the fairing on the flow near the wing-plate junction (The picture on the right shows the small fairing)

Nowhere a vortex was found with this tuft.

With the small fairing, comparable results were obtained as with the large fairing. The boundary layer did not separate, which was again confirmed with the tuft. In conclusion it can be said that both these fairings satisfy in eliminating separation.

The boundary layer calculations showed that for a given fairing geometry the maximum value of the shape factor H increases when the Reynolds number is reduced, thus bringing the flow closer to separation, see Fig. 8 (upper). In these calculations, the starting conditions for Re_q were adapted as appropriate (see Fig. 4).

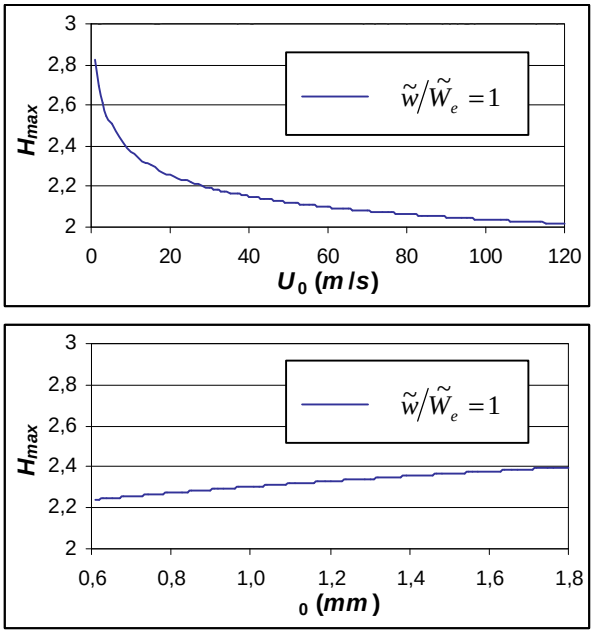

Figure 8: Small fairing separation predictions (When $\tilde{w}/\tilde{W}_e = u/U_e$ the flow separates)

Accordingly, it was tried during testing to induce separation on the small fairing by lowering the tunnel speed. However, no situation was found in which the fairing lost its function (i.e. the boundary layer separated), even by lowering the air speed that much ($U_\infty \approx$ 5 *m/s*) that the oil did not flow any more, whilst being at its thinnest solution.

Further calculations show that increasing the momentum loss thickness at the calculation starting point, cause an increase of the maximum value for the shape factor H as well, as can be seen in the lower graph of Fig.8, where U_∞ was kept constant at 20 *m/s*. This was also investigated in the windtunnel by applying thicker layers of zigzag tape. Again, the fairing did not loose its function.

It can therefore be concluded that the small fairing can be designed even more critically. In addition, it seems that the optimistic assumption (Eq. 6b) can be used with reasonable confidence to represent the flow-relieving effect in the prediction method for the boundary layer.

Now recall the second requirement the fairing has to fulfill, which is to promote a quick laminarization of the flow. As the flow proceeds on the fairing, the mass flow in the boundary layer decreases rapidly, until the condition is reached where the flow fluctuations cannot maintain their strength and die out, causing the flow to become laminar. By using a stethoscope tube, which responds to the pressure fluctuations in the flow, regions of laminar and turbulent flow can be discerned. The observations in the experiments agreed with the predictions from the boundary layer calculations. At an airspeed of 20 *m/s* it was found that the flow on the leading edge of the fairing was turbulent up to a height of approximately 25 *mm* above the flat plate (which is of the order of the original boundary layer height on the plate) and laminar above this height. As the streamlines downstream of the leading edge bend down (see Fig. 7, right), the upper side of turbulent wedge is at first almost horizontal. The lower point of transition on the leading edge and the fact that the streamlines bend down cause this fairing to fulfill its second design requirement, making the boundary layer on the wing laminar much closer to the root than is possible with a straight wing without fairing.

4 Conclusions and Recommendations

A design procedure for a wing-body fairing was presented, that is based on the calculation of the boundary layer development along the attachment line of the configuration. In its present form it is applied to a symmetrical flow geometry and makes use of the corresponding simplifications. The computational effort is quite modest, which may make it a worthwhile

design method, which can serve as complementary or alternative to empirical or demanding CFD approaches.

The boundary layer calculation was further simplified by making an additional assumption regarding the cross-flow profile. Based on these results, two fairing geometries were realized and wind tunnel tests revealed that both fairings worked. As the small fairing had been designed with some safety margin, there seems to be a further optimization possible.

A logical next step in the development of the design method is to investigate to what extent a similar approach can be applied to non-symmetrical flow situations, to enable the design of a fairing for a cambered wing and / or under angle of attack.

Further attention may be given to an improved integration of the existing design procedure, in particular the coupling of the different computational modules which now still requires some intervention from the user, as well as a feedback of the boundary layer results when searching for the optimum fairing shape.

Finally, the behavior of the obtained fairing designs under off-design conditions needs to be determined, for example, to see whether the fairing shape remains functional under angle of attack. In addition, the performance of the fairing in terms of overall drag reduction needs to be assessed. Other fairing geometries may be considered as well.

References

[1] Maughmer M.D.: An experimental investigation of wing/fuselage integration. *AIAA paper 87-2937*, 1987.

[2] Devenport, W.J., Agarwal, N.K, Dewitz, M.B., Simpson, R.L., Poddar, K.: Effects of a fillet on the flow past a wing-body junction. *AIAA Journal*, Vol. 28, 1990, pp.2017-2024.

[3] Devenport, W.J., Simpson, R.L., Dewitz, M.B., Agarwal, N.K.: Effects of a strake on the flow past a wing-body junction. *AIAA-paper-91-0252*, 1991.

[4] Ölçmen, B.E., Simpson, R.L.: Influence of wing shapes on surface pressure fluctuations at wing-body junctions. *AIAA Journal*, Vol. 32, *No. 1*, 1994, pp 6-15.

[5] Green S.M., Whitesides J.L.: A method for designing leading-edge fillets to eliminate flow separation. *AIAA paper 2000-4527*, 2000.

[6] Cebeci T., Cousteix J.: *Modeling and Computation of Boundary-Layer Flows*, Horizons Publishing/ Springer Verlag (1999).

[7] Cumpsty, N.A., Head, M.R.: The calculation of three-dimensional turbulent boundary layers. Part I: Flow over the rear of an infinite swept wing. *Aero. Quart.*, Vol. 18, 1967, pp. 55-84. Part II: Attachment-line flow on an infinite swept wing. *Aero. Quart.*, Vol. 18, 1967, pp. 150-164. Part III: Comparison of attachment-line calculations with experiment. *Aero. Quart.*, Vol. 20, 1968, pp. 99-113.

[8] Head, M.R.: Entrainment in the turbulent boundary layer. *ARC R. & M. 3152*, 1958.

[9] Van Oudheusden, B.W., Steenaert, C.B., Boermans, L.M.M.: A simple approach for the design of a wing-body fairing. *CEAS Aerospace Aerodynamics Research Conf.*, 10-12 June 2002, Cambridge, paper 57.

[10] Simpson, R.L.: Junction flows. *Ann. Rev. Fluid Mech.*, Vol. 33, 2001, pp. 415-443,

[11] Pfenninger, W.: Laminar flow control – Laminarization. In: *Special course on concepts for drag reduction*. *AGARD Report No.654*, 1977.

[12] Narasimha, R., Sreenivasan, K.R.: Relaminarization of fluid flows, *Adv. Appl. Mech.*, Vol. 19, 1979, pp. 221-309.

[13] White, F.M.: *Viscous fluid flow*, 2nd ed. McGraw-Hill, 1991.

[14] Gaster, M.: On the flow along swept leading edges, *Aero. Quart.*, Vol. 18, 1967, pp. 165-184.

[15] Poll, D.I.A.: Transition in the infinite swept attachment line boundary layer, *Aero. Quart.*, Vol. 30, 1979, pp. 607-629.

[16] Pfenninger, W.: Some results from the X-21 program. Part I. Flow phenomena at the leading edge of swept wings. *AGARDograph 97*, 1965.

[17] Spalart, P.R.: Direct numerical study of leading-edge contamination, In: *Fluid dynamics of three-dimensional turbulent shear flows and transition. AGARD-CP*-438, 1989..

[18] Abbott, I.H., Von Doenhoff, A.E.: *Theory of Wing Sections.* McGraw-Hill, 1949.

[19] Kubrynski, K.: Design of 3-dimensional complex airplane configurations with specified pressure distribution via optimization. In: *Proc. ICIDES III Conference*, G.S. Dulikravich, Washington DC, 1991.